THE JOURNAL OF BIOLOGICAL CHEMISTRY VOL. 287, NO. 34, pp. 28943–28955, August 17, 2012

X-linked Sideroblastic Anemia Due to Carboxyl-terminal ALAS2 Mutations That Cause Loss of Binding to the β-Subunit of Succinyl-CoA Synthetase (SUCLA2)*[S]

Received for publication, June 4, 2012 Published, JBC Papers in Press, June 27, 2012, DOI 10.1074/jbc.M111.306423

David F. Bishop[‡1], **Vassili Tchaikovskii**[‡], **A. Victor Hoffbrand**[§], **Marie E. Fraser**[¶], **and Steven Margolis**[‡]

From the [‡]*Department of Genetics and Genomic Sciences, Mount Sinai School of Medicine, New York, New York 10029, the* [§]*Department of Haematology, Royal Free Hospital, London NW3 2QG, United Kingdom, and the* [¶]*Department of Biological Sciences, University of Calgary, Calgary, Alberta T2N 1N4, Canada*

Background: Disease-causing missense mutations typically yield enzymes with significantly reduced catalytic activity or stability.
Results: Two mutant ALAS2 enzymes causing X-linked sideroblastic anemia had normal enzymatic activity but failed to bind to the β subunit of succinyl-CoA synthetase.
Conclusion: Thus, this interaction may play a critical role *in vivo*.
Significance: This is the first report of the loss of succinyl-CoA synthetase binding for ALAS2 mutations in X-linked sideroblastic anemia.

Mutations in the erythroid-specific aminolevulinic acid synthase gene (*ALAS2*) cause X-linked sideroblastic anemia (XLSA) by reducing mitochondrial enzymatic activity. Surprisingly, a patient with the classic XLSA phenotype had a novel exon 11 mutation encoding a recombinant enzyme (p.Met567Val) with normal activity, kinetics, and stability. Similarly, both an expressed adjacent XLSA mutation, p.Ser568Gly, and a mutation (p.Phe557Ter) lacking the 31 carboxyl-terminal residues also had normal or enhanced activity, kinetics, and stability. Because ALAS2 binds to the β subunit of succinyl-CoA synthetase (SUCLA2), the mutant proteins were tested for their ability to bind to this protein. Wild type ALAS2 bound strongly to a SUCLA2 affinity column, but the adjacent XLSA mutant enzymes and the truncated mutant did not bind. In contrast, vitamin B6-responsive XLSA mutations p.Arg452Cys and p.Arg452His, with normal *in vitro* enzyme activity and stability, did not interfere with binding to SUCLA2 but instead had loss of positive cooperativity for succinyl-CoA binding, an increased K_m for succinyl-CoA, and reduced vitamin B6 affinity. Consistent with the association of SUCLA2 binding with *in vivo* ALAS2 activity, the p.Met567GlufsX2 mutant protein that causes X-linked protoporphyria bound strongly to SUCLA2, highlighting the probable role of an ALAS2-succinyl-CoA synthetase complex in the regulation of erythroid heme biosynthesis.

In humans, the rate-limiting enzyme for erythroid heme biosynthesis is encoded by the X-linked gene, 5-aminolevulinate synthase (*ALAS2*[2]; EC 2.3.1.37). The enzyme is expressed only in fetal liver and adult bone marrow to support hemoglobin synthesis (1). Its translation from mRNA is regulated by iron, and it functions in the mitochondria following import from the cytoplasm and cleavage of an amino-terminal signal sequence that specifies mitochondrial targeting (2). The formation of 5-aminolevulinic acid (ALA) from succinyl-CoA and glycine requires a vitamin B6 cofactor, pyridoxal 5′-phosphate (PLP), that is covalently bound to human ALAS2 Lys-391 (3, 4).

X-linked sideroblastic anemia (XLSA), the most common congenital sideroblastic anemia, is caused by ALAS2 mutations that compromise its activity, stability, or mitochondrial localization (5–7). The resulting heme deficiency causes decreased hemoglobin and increased iron stores with the clinical manifestations of pallor, fatigue, weight loss, and cardiac failure or diabetes due to secondary toxicity from iron overload (2). The severity of the disorder (neonatal to late onset) depends primarily on the amount of residual ALAS2 mitochondrial enzyme activity. Structural and functional studies of pure wild type and mutant ALAS2 have been facilitated using prokaryotic overexpression of a fusion protein to stabilize and solubilize the enzyme (8, 9). Of all of the XLSA coding mutations, only p.Arg452Cys and p.Arg452His have been found to display normal ALAS2 enzymatic activity and thermostability *in vitro*, suggesting that some other factor reduced ALAS2 activity *in vivo* (10). To date, at least 61 different ALAS2 mutations have been discovered in 103 separate pan-ethnic XLSA kindreds (11–14).[3] The disorder is often responsive to vitamin B6 therapy

* This work was supported, in whole or in part, by National Institutes of Health Grant R01DK40895. This work was also supported by New York State Department of Health Research Grant C024404 and a Discovery Grant from the Natural Sciences and Engineering Research Council of Canada.
[S] This article contains supplemental Table S1.
[1] To whom correspondence should be addressed: 1425 Madison Ave., New York, NY 10029. Tel.: 212-659-6795; Fax: 212-849-2508; E-mail: david.bishop@mssm.edu.

[2] The abbreviations used are: ALAS2, 5-aminolevulinate synthase, erythroid isozyme; ALA, 5-aminolevulinic acid; MBP, maltose-binding protein; pMALc2, prokaryotic expression vector for cytoplasmically expressed MBP fusion protein; PLP, pyridoxal 5′-phosphate; SUCLA2, *H. sapiens* succinyl-CoA synthetase ADP-forming β subunit; XLSA, X-linked sideroblastic anemia; XLP, X-linked protoporphyria; SCS, succinyl-CoA synthetase; MBP, maltose-binding protein; SCL2, MBP-SUCLA2 fusion protein.
[3] D. F. Bishop and A. May, unpublished observations.

coupled with phlebotomy or chelation therapy to remove excess iron (11, 15, 16).

Recently, a new role for ALAS2 was discovered. Deletion/frameshift mutations encoding the carboxyl-terminal region of ALAS2 caused protoporphyrin IX overproduction, rather than heme deficiency, leading to X-linked protoporphyria (XLP) with cutaneous photosensitivity (17). XLP was classified as a gain-of-function disorder because ALAS2 activity was greatly increased in crude extracts of recombinantly expressed XLP mutant enzymes.

In this report, we demonstrate that two unrelated XLSA patients with adjacent ALAS2 mutations in a specific region in the sequence of the carboxyl terminus (p.Met567Val and p.Ser568Gly) have enzymes with normal activity, stability, and kinetics but are unable to bind to SUCLA2, the β subunit (ATP-binding form) of succinyl-CoA synthetase. In contrast, the ALAS2 mutant enzyme (p.Arg452Cys), also with normal *in vitro* activity, binds to SUCLA2 but has lost positive cooperativity with succinyl-CoA binding and has reduced affinity for succinyl-CoA and PLP.

The novel finding that the p.Met567Val and p.Ser568Gly mutations caused XLSA and disruption of binding to SUCLA led to the question of why a different mutation in one of these residues (p.Met567GlufsX2) led to ALA overproduction and XLP (17). Here, we show that this mutant protein still binds strongly to SUCLA2, consistent with the observed enhanced activity of ALAS2 *in vivo*.

These studies provide new insights into the functional roles of certain carboxyl-terminal ALAS2 residues, identifying a region critical for the formation of an ALAS2·succinyl-CoA synthetase (SCS) enzyme complex that presumably is required for normal heme biosynthesis in mitochondria, the disruption of which was caused by adjacent carboxyl-terminal mutations in two XLSA patients.

EXPERIMENTAL PROCEDURES

Patients—The proband was a 40-year-old male who developed symptoms at 13 years of age. He was first seen at the Royal Free Hospital at age 14, when he was found to be pale and thin but of normal growth and intelligence. He was anemic with a hemoglobin of 8.5 g/dl, hematocrit 29.8%, 5.15×10^{12} red cells/liter, a mean cell volume of 57 fl, mean cell hemoglobin concentration of 16.7 pg, reticulocytes 3.1%, white cells 5.6×10^9/liter with a normal differential, platelets 315×10^9/liter, elevated serum iron of 48.5 mmol/liter, and a total iron binding capacity of 51 mmol/liter. Hemoglobin electrophoresis and liver function tests were normal, as were serum B12 and folate. Liver and spleen were not palpable. A bone marrow aspirate showed normoblastic hyperplasia with reversal of the myeloid erythroid ratio and greatly increased iron stores. The majority of the normoblasts were ringed sideroblasts. The blood film showed a dimorphic, anisocytic picture, with many of the cells being hypochromic, including pencil cells and target cells. His parents had normal blood counts as did a sister, aged 10. There was no obvious anemia in any of his relatives.

He was treated with pyridoxine up to a dose of 100 mg daily and in addition was treated from age 15 to 16 with gentle venesections to reduce his iron stores. By age 23, his hemoglobin had risen to around 9.4 g/dl, but he was found to have a serum ferritin of 1,080 μg/liter and again was placed on a regimen of gentle venesections.

Reagents—Deoxyribonuclease 1 (DNase) Type II, ribonuclease A (RNase) Type XII-A, PLP, succinyl-CoA sodium salt, acrylamide/bisacrylamide, 2-mercaptoethanol, BSA, PMSF, pepstatin A, leupeptin, and aprotinin were from Sigma; Precision Plus Protein™ unstained standards were from Bio-Rad; glycerol, glycine, mono-and dibasic potassium phosphate, electrophoresis grade disodium EDTA, DTT, ampicillin, and enzyme grade HEPES were from Fisher; ethylacetoacetate was from Fluka; acetylated BSA was from Ambion; Superose-12 was from GE Healthcare; MetaPhor® agarose was from FMC BioProducts; and Next Gel 10% solution for SDS-PAGE of proteins was from Amresco. The pMAL-c2 and c4X prokaryotic expression vectors, maltose-binding protein (MBP), factor Xa, amylose resin, 100-bp DNA ladder, T4-DNA-ligase, the Quick Ligation Kit, and restriction enzymes were purchased from New England Biolabs. Plasmid mini and midi prep kits, the DNA gel extraction kit, and HotStarTaq® master mix were from Qiagen. The QuikChange XL site-directed mutagenesis kit and BL21 CodonPlus-RP strain competent cells were from Stratagene. Top 10F competent cells were from Invitrogen. *Homo sapiens* succinate-CoA ligase ADP-forming β subunit DNA was from OriGene Technologies.

Mutation Detection in the Proband and Carriers—Genomic DNA from white blood cells of whole blood from the proband and family members was obtained at the Royal Free Hospital with informed consent and used at Mt. Sinai as template for mutation detection by PCR amplification of the regions of interest using primers listed in supplemental Table S1. For the proband, DNA sequencing of the promoter region, all exons, and all exon-intron boundaries was used to identify the specific mutation. DNA samples isolated from a normal individual, the proband, and his mother, sister, and two daughters were PCR-amplified, digested with NlaIII, and analyzed by agarose gel electrophoresis. DNA from normal individuals has NlaIII restriction fragments sized 33, 120, and 166 bp, whereas carrier heterozygotes have these restriction fragments for the wild type allele plus an additional 33 + 166 = 199-bp fragment due to the mutation, which ablates the restriction site on the mutant allele.

Site-directed Mutagenesis of ALAS2—All ALAS2 mutants were derived from pMALc2-AE2 (8) by site-directed mutagenesis using the Stratagene XL site-directed mutagenesis kit with appropriate primers (supplemental Table S1). Plasmid DNA was purified from XL1-Blue or DH5α transformed cells, and the final constructs were transformed into the *Escherichia coli* BL21 Codon Plus-RP strain (Stratagene). Positive clones for point mutations resulting in missense mutations p.Met567Val, p.Ser568Gly, and p.Arg452Cys/His were identified by restriction analysis using BspHI, HphI, and HhaI, respectively, and confirmed by sequence analysis of the XhoI to EcoRI fragment at the 3′-end of the ALAS2 construct. This region was then excised and recloned into XhoI/EcoRI-cut wild type pMALc2-AE2, and the junction sequences were confirmed by sequencing. For the 3′-truncation mutant, p.Phe557Ter, the XhoI region to the 3′-end of the ALAS2 coding sequence was PCR-amplified using a 3′-primer with a sequence matching that

prior to Asn-556 followed by a stop codon and including an EcoRI site. This amplicon was also XhoI/EcoRI-digested and cloned into the parent pMALc2-AE2 construct, and the sequence was confirmed.

Expression and Purification of ALAS2—Glycerol stocks of wild type or mutant *ALAS2* transformants were used to seed three 5-ml cultures, in Luria-Bertani (LB) medium (containing 100 μg/ml ampicillin), that were incubated at 37 °C overnight with shaking. The following day, these cultures were added to 1 liter of LB medium containing 0.2% glucose, 100 μg/ml ampicillin, and 10 μM PLP and grown at 37 °C in a gyratory shaker to a density of 0.6–0.8 A_{600}. After the addition of isopropyl β-D-thiogalactopyranoside to a concentration of 1 mM, growth with shaking was continued for 3 h at 37 °C. The cells were harvested in four 250-ml polycarbonate bottles by centrifugation at 6,000 × *g* for 20 min at 4 °C. The supernatants were discarded, and each pellet was resuspended in 5 ml of freshly prepared, sterile-filtered ice-cold lysis buffer containing 200 mM NaCl, 50 mM potassium HEPES, pH 7.4, 5 mM DTT, 1 mM EDTA, 0.4 mM PMSF, 200 μg/ml lysozyme, 10 μM PLP, 0.02% sodium azide, including additives: 1.0 μg/ml pepstatin A, 1.8 μg of aprotinin, 0.5 μg/ml leupeptin, 50 μl of 1 M $MgCl_2$, 200 μl of 5 mg/ml DNase, and 100 μl of 5 mg/ml RNase. After careful dispersion of each pellet in small aliquots of lysis buffer, the smooth suspensions were pooled, an additional 30 ml of lysis buffer was added, and the suspension was frozen at −80 °C until the next step.

Typically, the purification was continued on the next day by thawing in lukewarm water with swirling followed by storage on ice once the lysate was fully thawed. Cell debris was removed by 30 min of centrifugation at 27,000 × *g* at 4 °C. Half of the crude extract supernatant (25 ml) was slowly applied to an amylose resin column (2.8-cm diameter × 6 cm), equilibrated with lysis buffer excluding the above additives. After collection of the flow-through, the affinity chromatography column was washed with 40–50 ml of lysis buffer (minus additives), followed by 40 ml of 2× modified lysis buffer (modified by omission of additives). The MBP-ALAS2 fusion protein was eluted with 35 ml of 10 mM maltose in 1× modified lysis buffer. The first 5 ml was discarded, and 30 ml of eluate, containing the fusion protein, was collected. The regenerated column was then reloaded with the remaining 25 ml of crude extract, and the procedure was repeated. The fusion protein in the pooled eluates was concentrated by precipitation between 25 and 55% of saturation with ammonium sulfate and collected by centrifugation for 30 min at 27,000 × *g*. Precipitation was at 4 °C with equilibration for 30 min at each concentration of ammonium sulfate.

For Factor Xa cleavage of the recombinant MBP-ALAS2 fusion protein, the ammonium sulfate pellet was gently dissolved in cleavage buffer containing 100 mM NaCl, 50 mM potassium HEPES, 2 mM $CaCl_2$, 0.5 mM DTT, and 10 μM PLP and then adjusted to pH 8.0 with 1 N sodium hydroxide. The final volume was about 3 ml, and protein concentration was around 20–30 mg/ml. The MBP-ALAS2 protein complex was cleaved overnight by Factor Xa (2.5 μg of Factor Xa per 1 mg of MBP-ALAS2) at room temperature. The digested product was applied to a second amylose resin column (2.8-cm diameter × 3.5 cm) and was washed through the column with 20 ml of 1× lysis buffer, followed by concentration by ammonium sulfate precipitation at 55% of saturation. The protein pellet was redissolved in 2 ml of gel filtration buffer (50 mM NaCl, 50 mM potassium HEPES, 5 mM DTT, 0.4 mM PMSF, 10 μM PLP, and 0.02% NaN_3, adjusted to pH 7.4) and was applied onto two tandem (1.6 × 51-cm) FPLC columns containing Superose 12 gel filtration medium (GE Healthcare) that had been freshly washed overnight with gel filtration buffer. The FPLC column flow-rate was 0.2 ml/min, and the peak fractions were collected in 1-ml aliquots with monitoring by absorption at 280 nm, pooled, and concentrated using a Centriprep YM-50 ultrafilter (Millipore). Enzyme purity was assessed by SDS-PAGE of protein from each purification step alongside Bio-Rad Precision Plus Protein standards. Polyacrylamide gels were prepared using 10% ProPure Next Gel and ProPure 20X running buffer from Amresco (Solon, OH). The polyacrylamide gels were stained for 30 min on a gyratory shaker (~40 rpm) in a solution of 0.1% Coomassie Brilliant Blue G dye (Sigma) in a solution of 50% methanol and 10% glacial acetic acid in water. The gel was then destained for 15 min in this solution minus dye followed by overnight destaining in 12.5% methanol and 2.5% glacial acetic acid in water. Storage was in distilled water containing 0.02% sodium azide for increased contrast. Gels were air-dried between two pieces of cellophane (DryEase™, Invitrogen) in a stretching frame prior to digitization using an Agfa Duoscan scanner.

ALAS2 Enzyme and Protein Assays—Recombinant ALAS2 enzymatic activity was determined colorimetrically with modified Ehrlich's reagent (18). The 0.5-ml reaction volume contained 100 mM glycine, 50 mM potassium HEPES, pH 7.4, 10 mM $MgC1_2$, 1 mM DTT, 100 μM succinyl-CoA, 10 μM PLP, and 10–200 units of ALAS2 activity. Following incubation at 37 °C for 5 min, the reaction was terminated by the addition of 100 μl of 50% trichloroacetic acid, incubated 15 min on ice, and centrifuged for 10 min at 10,000 × *g*. A portion of the supernatant (400 μl) was mixed with 550 μl of 1 M sodium acetate, 30 μl of glacial acetic acid, and 50 μl of ethylacetoacetate in 12 × 75-mm glass tubes, capped with glass marbles, and placed in a boiling water bath for 10 min. After cooling on ice to room temperature, 1 ml of modified Ehrlich's reagent (18) was added, and the absorbance was measured at 554 nm within 10 min. Ehrlich's reagent was made fresh every week by diluting 42 ml of glacial acetic acid with 3 ml of distilled water, adding 10 ml of 70% perchloric acid to 1.0 g of dimethylaminobenzaldehyde and 175 mg of powdered $HgCl_2$ with magnetic stirring in a 100-ml beaker, adding the diluted acetic acid solution to the dissolved solids and adding water to a final volume of 55 ml. The molar extinction coefficient for the ALA-ethylacetoacetate-dimethylaminobenzaldehyde adduct is taken to be 7.2×10^4, as determined by Mauzerall and Granick (19). One unit of activity is that amount of enzyme required to catalyze the production of 1 nmol of 5-aminolevulinate per hour under the conditions of the assay.

Protein concentrations were determined by a modification of the fluorescamine method (20). The fluorescamine assay was standardized with BSA in the range of 1–15 μg of protein/assay. For comparison with other protein assays, the ratio of homogeneous ALAS2 fluorescamine protein to Bradford protein (Bio-

Rad) was determined to be 1.11, and the ratio of fluorescamine protein to micro-Lowry protein (1:5 dilutions of reagents A and B) was 0.64.

K_m Determinations—Each assay contained 1–2 μg of wild type or mutant ALAS2 enzyme. The glycine concentrations were varied from 2.5 to 50 mM at a succinyl-CoA concentration of 100 μM. The succinyl-CoA concentrations were varied from 10 to 100 μM at a glycine concentration of 100 mM. K_m values were calculated from Lineweaver-Burk and Eadie-Hofstee plots. Cooperativity was evaluated using Hill plots with V_{max} estimates obtained from Lineweaver-Burk plots. Subsequent Lineweaver-Burk plots using $1/S^{Hill\ n}$ were used to iteratively calculate revised V_{max} estimates until the Hill n value did not change further.

PLP Binding Kinetics of the ALAS2 Apoenzymes—The apoenzymes of wild type and mutant ALAS2 were prepared by overnight incubation at 4 °C at a protein concentration of 3 mg/ml in 5 mM hydroxylamine, 0.25 M potassium phosphate buffer, pH 7.4, containing 100 μM DTT and 1 mM EDTA (21). This was followed by Sephadex G-50 gel filtration (0.8 × 9 cm) in 50 mM potassium HEPES, pH 7.4, and 0.1 mM DTT. The apoenzymes were then concentrated by YM-50 centrifugal ultrafiltration (Millipore). The conversion to apoenzyme was monitored spectrophotometrically using a Hewlett/Packard model 8453 UV-visible system over the range of 250–450 nm. Reconstitution of 3 μg of apoenzyme in 10 μM PLP was monitored by enzymatic activity after preincubation for various times in the presence of 0.25 mg/ml acetylated BSA. For kinetic analyses, the apoenzyme preparations were titrated with increasing concentrations of PLP. The data were analyzed using Lineweaver-Burk, Eadie-Hofstee, and Hill plots in the same manner as for substrates kinetics.

Subcloning, Expression, and Purification of Human SUCLA2—The cDNA clone for the ADP-forming β subunit of succinyl-CoA synthetase (EC 6.2.1.5; succinate-CoA ligase (ADP-forming); SUCLA2) was purchased from OriGene Technologies and transformed into *E. coli* strain Top10. The *SUCLA2* coding region was amplified from the purified plasmid DNA using an XmnI-tailed sense primer and an EcoRI-tailed antisense primer (supplemental Table S1). The PCR product of 2,152 bp was digested with XmnI and EcoRI, followed by ligation into XmnI and EcoRI-cut pMAL-c4X, and transformed into BL21 Codon Plus-RP competent cells. The cDNAs of obtained colonies were subjected to PCR screening with oligonucleotides (supplemental Table S1) corresponding to sequences that are located in *pMAL c4* just before and after the cloning site and characterized by electrophoresis in 0.7% agarose gels. Restriction analysis with HindIII and electrophoresis in 2% MetaPhor agarose confirmed the presence of the fragment sizes expected for *SUCLA2* cDNA. The final selected clone was confirmed by sequence analysis of the entire coding region.

Expression and purification of the MBP-SUCLA2 fusion protein was similar to that of ALAS2 above and used previously established optimal buffer conditions (22) but omitted the cleavage and final Superose 12 gel filtration steps. Four tubes, each containing 5 ml of LB medium with 100 μg/ml ampicillin, were started from a glycerol stock of the *SUCLA2*-transformed cells with shaking at 37 °C overnight. The next day, this culture was seeded into 1 liter of LB SuperBroth (60 g/liter), containing 100 μg/ml ampicillin and 0.2% glucose. Cells were grown in a gyratory shaker to 0.9–1.0 A_{600}. After the addition of isopropyl β-D-thiogalactopyranoside to a concentration of 1 mM, growth was continued for 4–5 h at 37 °C. The cells were harvested as for MBP-ALAS2 expression and suspended in lysis buffer containing 100 mM KH_2PO_4, pH 7.4, 150 mM KCl, 5 mM sodium succinate, 1.0 mM EDTA, 0.02% NaN_3, and the additives 1.0 mM PMSF, 200 mg/ml lysozyme, 2 μg/ml leupeptin, 2 μg/ml pepstatin A, 1.8 μg/ml aprotinin, 200 μl of 10 mg/ml DNase, 100 μl of 5 mg/ml RNase, and 50 μl of 1 M $MgCl_2$. The suspension was frozen at −80 °C, and the purification was typically continued on the next day. Cell debris was removed from the thawed lysate by a 30-min centrifugation at 30,000 × *g*. The supernatant (crude extract) was subjected to affinity chromatography over an amylose resin column (2.8 × 6 cm), equilibrated with lysis buffer minus additives. The MBP-SUCLA2 fusion protein was eluted with 35 ml of 10 mM maltose in lysis buffer minus additives. The eluates were pooled and concentrated by precipitation on ice with stirring for 30 min with ammonium sulfate added to 65% of saturation. After centrifugation, the pellet was resuspended in 50 mM potassium HEPES, 150 mM NaC1, 1 mM EDTA, and 0.8 mM PMSF, adjusted to pH 7.4 by potassium hydroxide.

Binding of Human ALAS2 by Immobilized SUCLA2—Amylose resin columns (0.8-cm diameter × 1.7 cm) were equilibrated with lysis buffer, loaded with ~1 mg of affinity-purified MBP-SUCLA2 fusion protein each, and washed with four column volumes of gel filtration buffer. The amount of bound fusion protein (~1.6 nmol) was calculated by quantitating the unbound protein in the flow-throughs and washes and subtracting from the applied protein quantity. Wild type or mutant FPLC-purified ALAS2 (~1.9 nmol) was loaded on separate columns, followed by a 15-min incubation at room temperature. Unbound enzyme was eluted by washing with three volumes of gel filtration buffer, and the ALAS2 enzymatic activity in the flow-through and wash fractions was quantitated. The maltose-eluted fractions were assayed for ALAS2 activity and compared with the units of enzyme applied to the column.

For recovery of sufficient eluted proteins to analyze by SDS-PAGE, larger columns were used (0.8 × 2.5 cm), and 3 mg of MBP-SUCLA2 fusion protein was applied as affinity ligand. After washing, an excess of FPLC-purified wild type or mutant purified ALAS2 was applied, followed by another wash. The bound material was eluted by the addition of 10 mM maltose, which eluted both the MBP-SUCLA2 fusion protein and any components of the ALAS2 preparation that had been bound to it. The applied and eluted proteins were concentrated by centrifugal ultrafiltration and characterized by electrophoresis on 10% Pro-Pure Next Gel (Amresco) SDS-polyacrylamide gels alongside Bio-Rad Precision Plus Protein standards. Gels were passively air-dried between two pieces of cellulose film and digitized.

Binding of the Human SCS Holoenzyme by Immobilized Wild Type or M567V Mutant ALAS2—The reverse of the previous affinity binding experiment was accomplished by immobilizing ALAS2 instead of SUCLA2. The mature, recombinant human SCS α subunit, SUCLG1, was engineered to begin at the amino-

terminal sequence MSYTASRQHLY and end with the His tag-modified sequence, KRKMLAAALEHHHHHH, yielding a calculated subunit molecular mass of 33.5 kDa. The mature human SCS β subunit was engineered to begin with the amino-terminal sequence MSLHEYMSME, yielding a calculated subunit molecular mass of 44.6 kDa. Both subunits were co-expressed in *E. coli*, and the holoenzyme was purified to near homogeneity with only a minor (~9%) contaminant of about 60 kDa.[4] The wild type and M567V mutant MBP-ALAS2 fusion proteins were purified to homogeneity as described above and modified only by omission of the Factor Xa cleavage step.

Amylose resin columns (0.8-cm diameter × 2.5 cm) were equilibrated with lysis buffer, loaded with ~1 mg of wild type or M567V MBP-ALAS2 fusion protein each as the affinity ligand. After washing, an excess of SCS was applied, followed by another wash. The bound material was eluted by the addition of 10 mM maltose, which eluted both the MBP-ALAS2 fusion protein and any components of the SCS preparation that had been bound to it. The applied and eluted proteins were concentrated by centrifugal ultrafiltration and characterized by electrophoresis on 10% SDS-polyacrylamide gels as described above.

RESULTS

Identification of a Novel Exon 11 Mutation in a Patient with XLSA—DNA was purified from blood samples obtained with informed consent from the proband and family members. DNA sequencing of 1 kb of the promoter, the intron/exon boundaries, all exons, and 300 bp of 3′-flanking sequence was performed as described previously (11), and the only mutation present was c.1699A→G in exon 11, encoding a valine substitution for methionine at codon 567 (p.Met567Val). The mutation eliminated an NlaIII site, facilitating carrier analysis in family members. As shown in Fig. 1, the proband's unaffected mother, sister, and two daughters were carriers. The proband and all carriers were negative for the p.Cys282Tyr hemochromatosis mutation, and only his daughters were heterozygous for the p.His63Asp hemochromatosis allele (data not shown). The 1000 Genomes Project did not report any polymorphisms corresponding to this mutation.

Expression, Purification, and Enzymatic Activities of Wild Type and Mutant ALAS2—Large amounts of pure wild type and mutant ALAS2 were obtained for comparisons of properties, by expression of the enzymes as fusion proteins with the *E. coli* MBP (9). Previous studies in this laboratory had shown that expression of native human ALAS2 in bacteria resulted in large amounts of inclusion bodies but that the fusion protein with the attached highly soluble MBP was active and soluble, facilitating purification by amylose affinity chromatography. Subsequent removal of the MBP moiety by Factor Xa resulted in the native, mature mitochondrial form with an amino-terminal Asp-79. Wild type, p.Met567Val, and additional mutant ALAS2 enzymes were purified to homogeneity in three steps, as described under "Experimental Procedures," resulting in milligram quantities of enzyme from 1 liter of culture in an about 25% yield (Table 1). The purity of the wild type enzyme preparation at each step of purification is shown in Fig. 2*A*, and that of the purified mutant enzymes is shown in Fig. 2*B*. Despite extensive use of protease inhibitors and removal of Factor Xa by chromatography following the digestion step, two SDS-polyacrylamide gel bands were always observed for the post-FPLC ALAS2 enzymes, except for a 49.5-kDa truncation mutant, demonstrating that the proteolytically sensitive site was near the terminal Asn-556 residue of this mutant. The specific activity of each enzyme was always the same regardless of the ratio of the two forms, indicating that both ALAS2 forms were fully active. This carboxyl-terminal proteolysis of recombinant ALAS2 previously had been noted by another research group (23). Mass spectrometric analysis of trypsin fragments generated from each of the four major bands in Fig. 2*A*, *lane 3*, identified the 59.5 kDa band as *E. coli* GroEL (also as previously observed) (23), the 51.7 and 49.5 kDa bands as human ALAS2, and the 42.2 kDa band as MBP (data not shown). For the 51.7 kb band (relative to SDS size standards), the minimal region present by identification of tryptic peptides by mass spectrometry was Ala-88 to Arg-572, predicting an expected size of at least 53.7 kDa. For the 49.5 kDa band, the Ala-88 to Asn-556 region confirmed to be present by peptide mass analysis and by the size of the truncation mutant predicted an expected size of 51.6 kDa.

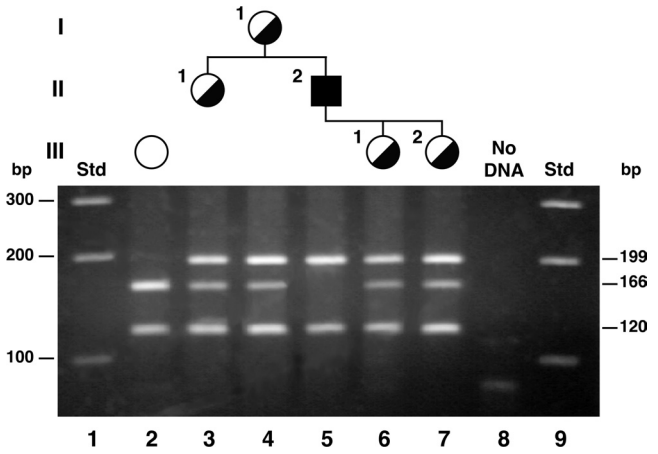

FIGURE 1. **Genotype analysis of the proband and family members.** DNA isolated from a normal individual, the proband, and his mother, sister, and two daughters was PCR-amplified, digested with NlaIII, and analyzed by agarose gel electrophoresis. *Lanes 1* and *9*, molecular weight standards; *lane 8*, a no-template PCR control; *lane 2*, DNA from an unrelated normal control; *lanes 3–7*, digested DNAs from the proband's sister (*II*, *1*), mother (*I*, *1*), male proband (*II*, *2*), and two daughters (*III*, *1*&*2*), respectively. The *lane 2* control shows the expected 120- and 166-bp NlaIII fragments, with the additional 33-bp fragment having migrated below the picture frame. *Lane 5* shows the 120-bp fragment and uncut 166 + 33 = 199 bp band for the hemizygote, whose mutation ablates the restriction site, whereas the *other lanes* contain all three bands, showing that all females in the pedigree are heterozygous carriers.

Purified ALAS2 tended to aggregate if stored at too high concentrations at 4 °C, but it remained soluble with an unchanged two-banded pattern for at least 4 years when stored at −80 °C in 20% glycerol (Fig. 2*A*, *lane 5*). With storage at −20 to 4 °C for extended periods, small amounts of lower molecular weight bands could be seen on SDS gels (*e.g.* see Fig. 2*B*).

The Mutant p.Met567Val Enzyme Had Normal Enzyme Kinetics and Stability—The native wild type and mutant ALAS2 enzymes were cleaved from MBP, purified, and further

[4] M. E. Fraser, unpublished observations.

TABLE 1
Purification of recombinant wild type and mutant human ALAS2

ALAS2 enzyme	Step	Activity	Specific activity	Yield	Purification
		units	*units/mg*	*%*	*-fold*
Wild type	Crude extract	1,690,000	1,630	100	1
	Affinity chromatography	1,160,000	34,000	69	21
	Gel filtration	487,000	96,700	29	59
p.Met567Val	Crude extract	1,170,000	906	100	1
	Affinity chromatography	634,000	17,500	54	19
	Gel filtration	260,000	92,700	22	102
p.Ser568Gly	Crude extract	1,610,000	1,430	100	1
	Affinity chromatography	193,000	14,600	12	10
	Gel filtration	175,000	137,000	11	84
p.Phe557Ter	Crude extract	1,730,000	1,690	100	1
	Affinity chromatography	1,640,000	27,000	95	16
	Gel filtration	1,230,000	103,000	71	61
p.Arg452Cys	Crude extract	1,580,000	1,520	100	1
	Affinity chromatography	1,180,000	36,900	75	24
	Gel filtration	311,000	87,100	20	57
p.Arg452His	Crude extract	973,000	1,470	100	1
	Affinity chromatography	528,000	18,700	56	13
	Gel filtration	183,000	99,100	26	67

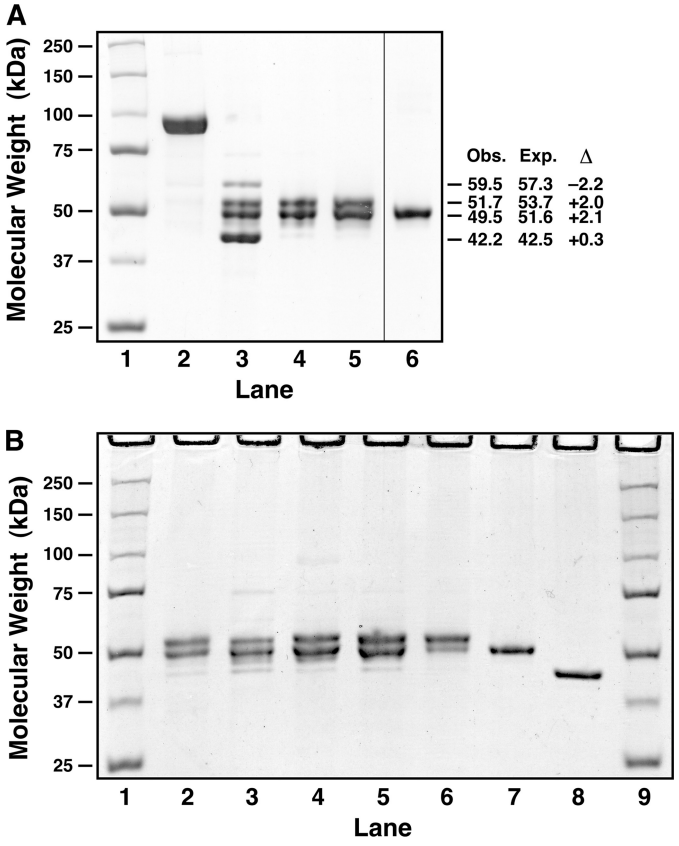

FIGURE 2. **SDS-PAGE analysis of ALAS2 purification products.** Protein size analysis of each step of the purification of recombinant human ALAS2 was done by denaturing polyacrylamide gel electrophoresis. *A*, *lanes 2–5*, wild type ALAS2. *Lane 1*, size standards; *lane 2*, affinity-purified MBP-ALAS2 fusion protein; *lane 3*, post-Factor Xa cleavage of fusion protein; *lane 4*, post-FPLC Superose gel filtration chromatography of the cleaved fusion protein; *lane 5*, same purification stage, sample stored at −80 °C for 3.75 years; *lane 6*, post-FPLC fraction of p.Phe557Ter enzyme (electrophoresed in the same gel, but intervening lanes excised). *Obs*., observed size estimated from the size markers; *Exp*., expected size calculated from peptide mass as discussed under "Results"; Δ, *Exp*. minus *Obs*. *B*, typical SDS-PAGE profiles of wild type and mutant ALAS2 proteins purified to the post-FPLC stage. *Lanes 1* and *9*, size standards; *lane 2*, wild type; *lane 3*, p.Arg452Cys; *lane 4*, p.Arg452His; *lane 5*, p.Met567Val; *lane 6*, p.Ser568Gly; *lane 7*, p.Phe557Ter; *lane 8*, MBP.

characterized by kinetic studies. The apparent K_m and V_{max} values for glycine and the K_m values for succinyl-CoA were essentially identical for the wild type and p.Met567Val enzymes (Table 2). As evidenced from linear Lineweaver-Burk and Hill plots (not shown), glycine substrate binding appeared to follow normal kinetics for both enzymes with a Hill number of ~1.0.

Previously, it had not been reported that ALAS2 is a homotropic allosteric enzyme that has positive cooperativity with succinyl-CoA substrate binding. This was demonstrated by upward curving Lineweaver-Burk plots as shown in Fig. 3*A* for the wild type enzyme. The Hill number of 1.7 determined by the slope of a Hill plot of $\log(v/V_{max})$ *versus* $\log S$ was consistent with the homodimeric structure of ALAS2, which could theoretically yield a maximum Hill number (n) of 2.0 for complete positive cooperativity. The linear Lineweaver-Burk form of the Hill equation plot (24) with the substrate concentration raised to the apparent Hill n power is shown in Fig. 3*B*. The p.Met567Val mutant's Hill number of 1.8 overlapped in S.D. value with the wild type value (Table 2), demonstrating that its positive cooperativity was unaffected by the mutation.

Although the homogeneous mutant p.Met567Val enzyme had normal kinetics, it was possible that it caused XLSA by being substantially less stable than the wild type enzyme. However, thermostability studies at 45 °C revealed that the mutant was as stable or more stable than wild type enzyme (Table 2). In summary, there was no evidence from enzyme kinetics or from protein stability that explained the observed X-linked sideroblastic anemia in the proband.

An Adjacent XLSA Mutation Behaved Similarly—To assess whether other mutations in this carboxyl-terminal region of ALAS2 might behave similarly, the adjacent p.Ser568Gly mutant ALAS2 previously reported to have 32% of wild type recombinant enzymatic activity (25) was constructed, expressed, purified, and characterized. As was the case for the p.Met567Val change, this change was also not a polymorphism as determined by its absence in the results of the 1000 Genomes Project. The pure enzyme displayed greater than wild type specific activity (137,000 units/mg; Table 1). Kinetic analysis revealed that nearly all of its properties were essentially the

TABLE 2
ALAS2 kinetics parameters

Parameter[a]	Wild type	p.Met567Val	p.Ser568Gly	p.Phe557Ter	p.Arg452Cys	p.Arg452His
SA (units/mg)[b]	97,000	93,000	137,000	103,000	87,000	99,100
V_{max} Gly (units/mg)	99,500 ± 625	106,000 ± 10,200	109,000 ± 21,000	173,000 ± 30,700	120,000 ± 4,860	130,000 ± 36,600
K_m Gly (mM)	10.2 ± 1.5	11.6 ± 2.0	5.7 ± 1.0	7.7 ± 3.0	15 ± 5	12.4 ± 8.0
n_{Hill} Gly	0.99 ± 0.02	0.99 ± 0.04	1.0	1.0	1.0	0.99 ± 0.11
K_m SucCoA (μM)	47.0 ± 5.0	41.4 ± 1.4	67.4 ± 19.1	36.3 ± 4.1	480 ± 120	76 ± 27
n_{Hill} SucCoA	1.7 ± 0.1	1.8 ± 0.1	2.0 ± 0.3	1.7 ± 0.12	1.2 ± 0.14	1.1 ± 0.16
K_a PLP (nM)[c]	27.8 ± 0.2	ND[d]	ND	ND	780 ± 200	868
$t_{½}$ 45 °C (min) (*n*)	23.2 ± 4.0 (5)	26.8 ± 0.5 (2)	24.6 ± 6.7 (2)	29.8 ± 0.5 (2)	22.9 ± 2.4 (3)	26.1 ± 3.0 (4)

[a] Data are means ± S.D. for $n = 3–4$ separate experiments except as indicated for the half-life data. For data with no S.D., $n = 1$.
[b] SA, specific activity as measured by the ALAS2 assay described under "Experimental Procedures."
[c] K_a PLP is defined as the apparent activation constant derived from an Eadie-Hofstee plot of PLP concentration *versus* activity at saturating concentrations of glycine and succinyl-CoA.
[d] ND, not determined.

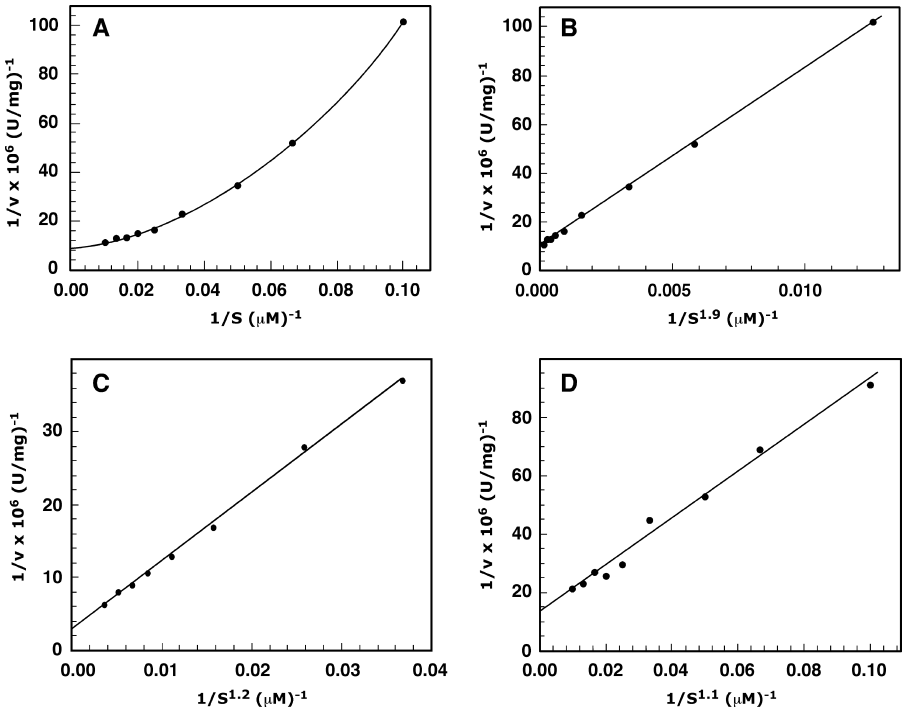

FIGURE 3. **Lineweaver-Burk plots of wild type and Arg-452 ALAS2 mutants.** Lineweaver-Burk plots were constructed for the 5-min end point reaction rates of wild type and mutant ALAS2 with varying concentrations of succinyl-CoA at 37 °C with glycine at 100 mM and the rest of the reaction conditions as described under "Experimental Procedures." The reactions were initiated by the addition of the succinyl-CoA to reaction tubes preincubated at 37 °C. *A*, wild type enzyme. *B*, wild type enzyme data plotted with the Hill transformation of the Lineweaver-Burk plot using $1/S^n$. Hill *n* was estimated iteratively using the Hill *n* derived from the slope of a plot of $\log(V_{max}/(1 - V_{max}))$ *versus* $\log S$ and recalculation of V_{max} from Lineweaver-Burk plots using $1/S^n$ until Hill *n* was constant. *C*, the Hill-transformed Lineweaver-Burk plot of reaction rate data for the p.Arg452Cys mutant enzyme. *D*, same as in C for the p.Arg452His mutant enzyme.

same as those of the wild type enzyme, including positive cooperativity with succinyl-CoA binding and thermostability (Table 2). Only the K_m for glycine was different, but it was lower than wild type, indicating even better affinity. Thus, this adjacent mutation in another patient with XLSA exhibited the same surprising result; it encoded a mutant enzyme with essentially normal enzyme kinetics and thermostability. Perhaps the previously reported recombinant ALAS2 specific activity was lower than that reported here due to the presence of the glutathione *S*-transferase fusion protein on the former construct or due to some other experimental differences.

Deletion of the ALAS2 Carboxyl Terminus Did Not Decrease ALAS2 Activity or Stability—Additional carboxyl-terminal ALAS2 mutations proximal to or including Met-567 have been reported in XLSA patients: p.Arg559His (26), p.Arg560His (16, 27), p.Val562Ala (14), and p.Met567Ile (14). To investigate if the carboxyl-terminal region that included these mutations was required for activity and stability *in vitro*, we analyzed the properties of a recombinant ALAS2 enzyme truncated (minus 31 residues) after residue Asn-556, similar in size to the apparently fully active proteolytic product observed after purification of the wild type enzyme. The truncated enzyme was purified in high yield (71%; Table 1) and had normal specific activity, positive cooperativity, normal K_m values for both glycine and succinyl-CoA, and slightly increased thermostability (Table 2). The truncated enzyme had a 1.7-fold higher V_{max} for glycine (Table 2) and a 1.9-fold higher V_{max} for succinyl-CoA (data not shown) than for wild type enzyme.

Other XLSA Mutations with Normal in Vitro Activity and Stability Had Altered Enzyme Kinetics—Previously, we had identified p.Arg452Cys as a causative mutation of XLSA by its occurrence in two unrelated XLSA families (11) and p.Arg452His in two unrelated families with pyridoxine-responsive XLSA (28, 29). Subsequently, Furuyama *et al.* (10) found

TABLE 3
SUCLA2 affinity chromatography of human wild type and mutant ALAS2

Component	Wild type ($n = 7$)	p.Arg452Cys ($n = 2$)	p.Met567Val ($n = 3$)	p.Ser568Gly ($n = 2$)	p.Phe557Ter ($n = 2$)
Immobilized SUCLA2 (nmol)	1.66 ± 0.74	2.31 ± 0.23	1.45 ± 0.48	2.87 ± 0.06	1.79 ± 0.31
Applied ALAS2 (nmol)	2.19 ± 0.56	3.03 ± 0.00	1.81 ± 0.71	2.87 ± 0.00	1.71 ± 0.04
ALAS2 in flow-through (nmol)	1.54 ± 0.50	1.39 ± 0.32	1.88 ± 0.52	2.81 ± 0.13	1.56 ± 0.09
ALAS2 bound/SUCLA2[a] (mol %)	39.9 ± 19.0	72.2 ± 20.9	6.42 ± 7.08	2.77 ± 3.91	8.28 ± 1.22
Difference from wild type (p)[b]		0.075	0.021**	0.034**	0.060

[a] Generally, a slight molar excess of ALAS was applied to the SUCLA column, so the percentage bound was calculated by subtracting the flow-through from the applied ALAS2 and dividing by the amount of immobilized SUCLA2. The values are the averages of the individual experiments.
[b] Probability of the binding of mutant ALAS2 to SUCLA2 being different from that of wild type binding using the unpaired Student's t test (**, significantly different from wild type).

that prokaryotically expressed p.Arg452Cys and p.Arg452His enzymes had normal activity, thermostability, and PLP binding and bound to the ATP-utilizing β subunit of succinyl-CoA synthetase (SUCLA2). They hypothesized that this mutation affected either dimerization or a protein-protein interaction with another protein. We confirmed that the purified enzymes (Table 1) have normal activities and thermostabilities under saturating substrate conditions but found that the affinities for succinyl-CoA binding for the p.Arg452Cys and p.Arg452His enzymes were 10- and 2-fold lower, respectively, than for wild type enzyme (Table 2). In addition, positive cooperativity with succinyl-CoA binding was nearly absent for both mutations, and the K_a values for PLP were increased (Table 2). Thus, kinetic analyses demonstrated that they were both defective in succinyl-CoA binding and cooperativity with an additional defect in cofactor binding, consistent with the observation that these patients were anemic and pyridoxine-responsive (10, 11, 28). The cooperative nature of succinyl-CoA binding was previously anticipated by both kinetic and structural studies that supported the conclusion that binding of this substrate promoted a conformational change (30, 31).

SUCLA2 Affinity Chromatography of ALAS2—Because the two exon 11 point mutations caused XLSA but did not significantly alter enzyme kinetics or stability, the possibility was explored that they disrupted the known interaction between ALAS2 and the beta subunit of the ATP-utilizing isozyme of succinyl-CoA synthetase (SUCLA2) (22). The MBP-SUCLA2 fusion protein was used as an affinity ligand to bind FPLC-purified wild type or mutant ALAS2. Approximately 40 and 70% of the wild type or p.Arg452Cys enzymes were bound to the SUCLA2 affinity columns, respectively, whereas only 6.4, 2.8, and 8.3% of the p.Met567Val, p.Ser568Gly, and p.Phe557Ter mutant ALAS2 enzymes were retained (Table 3). Because preparations of recombinantly expressed ALAS2 were mixtures of full-length and truncated enzyme subunits (*e.g.* see Fig. 2), the fact that a significant portion of the wild type ALAS2 did not bind was not unexpected.

Larger scale binding experiments permitted direct SDS-PAGE analysis of the enzyme forms after maltose elution of both the bound MBP-SUCLA2 and ALAS2 proteins from amylose affinity columns (Fig. 4). The MBP-SUCLA2 fusion protein migrated near the predicted size of 93 kDa, whereas lower amounts of smaller species, possibly proteolytic fragments, could also be seen (Fig. 4*A*, *lane 2*). When *E. coli* lysates from cultures lacking the MBP-SUCLA2 plasmid were applied, washed, eluted, and analyzed by PAGE, the extra bands were not seen (data not shown), indicating that the extra bands in

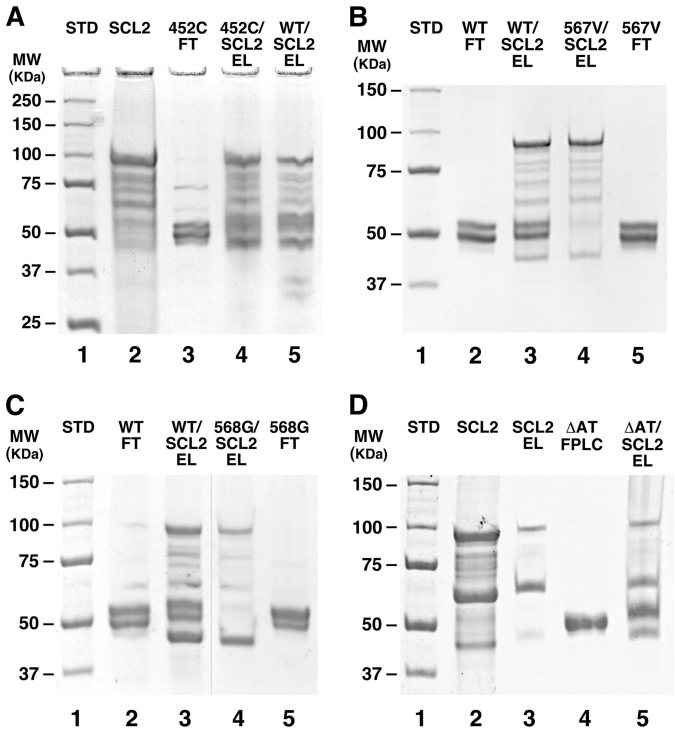

FIGURE 4. **SUCLA2 affinity chromatography of ALAS2.** Amylose resin columns were loaded with affinity-purified recombinant human MBP-SUCLA2 fusion protein (SCL2) and washed, and then aliquots of wild type and mutant post-FPLC purified ALAS2 enzyme preparations were applied, washed, and then eluted with maltose as described under "Experimental Procedures." *A*, SDS-PAGE of SCL2 and of WT and p.Arg452Cys ALAS2. *Lane 1*, molecular weight standards; *lane 2*, SCL2 after purification by amylose resin affinity chromatography; *lane 3*, flow-through fraction containing excess p.Arg452Cys protein that did not bind to the amylose/SCL2 affinity column; *lane 4*, material eluted by maltose from the amylose/SCL2 column to which the p.Arg452Cys protein had been loaded and washed; *lane 5*, material eluted from an amylose/SCL2 column to which wild type ALAS2 had been loaded and washed. Note that both SCL2 and bound ALAS2 are eluted in the material electrophoresed in *lanes 4* and *5*. *B*, similar to *A* but showing the wild type flow-through fraction in *lane 2* and the maltose-induced elution of the wild type enzyme along with SCL2 in *lane 3*. *Lane 4*, maltose-eluted material from an amylose/SCL2 column to which the p.Met567Val protein had been applied; *lane 5*, flow-through from that column during the p.Met567Val application step. Note that in contrast to the co-elution of SCL2 and ALAS2 bands in *lane 3* for the wild type enzyme, only SCL2 bands were eluted in *lane 4*, showing that no p.Met567Val protein was bound to SCL2. *C*, similar to *B*, showing again that wild type enzyme binds and is co-eluted with SCL2, whereas the mutant p.Ser568Gly protein does not bind (*lane 5*), and only SCL2 bands are eluted (*lane 4*). The *line* between *lanes 3* and *4* indicates an excised region of the gel. *D*, as in *A*; *lane 2*, amylose affinity resin-purified SCL2 protein before loading onto a second amylose column; *lane 3*, elution of that material by maltose. *Lane 4*, FPLC-purified p.Met567GlufsX1 protein resulting from the ΔAT *ALAS2* mutation; *lane 5*, co-elution of this mutant protein with SCL2, showing that unlike the p.Met567Val mutation, this mutation binds strongly to SCL2.

Fig. 4*A*, *lane 2*, were derived entirely from MBP-SUCLA2 and its degradation products, from MBP-SUCLA2 and other *E. coli* proteins that bound to it, or both.

Fig. 4*A*, *lane 3*, shows two bands in the flow-through fractions containing excess ALAS2 p.Arg452Cys protein that did not stick to the column, whereas *lanes 4* and *5* show the same two bands for mutant and wild type ALAS2 eluted by maltose from the amylose affinity column after the SUCLA2-bound columns were loaded with p.Arg452Cys and wild type enzyme, respectively.

In contrast, when mutant p.Met567Val protein was applied to the MBP-SUCLA2 affinity columns, it did not bind (Fig. 4*B*, *lane 4*) but rather was found only in the flow-through (*lane 5*). This confirmed the experiment based on recovery of enzymatic activity (Table 3) and conclusively demonstrated the loss of ALAS2 binding to SUCLA2 for the p.Met567Val mutation. In an identical manner, the p.Ser568Gly mutant ALAS2 protein also failed to bind to SUCLA2 (Fig. 4*C*, *lane 4*). Note that because ALAS2 is a dimeric enzyme and because the SUCLA2 affinity columns were run under native conditions, both the truncated and native wild type ALAS2 forms are retained due to binding of wild type/truncated heterodimers.

Although many repeated experiments confirmed these affinity column results, there were both variable amounts of contaminating bands in the less purified MBP-SUCLA2 preparations and variable amounts of binding to ALAS2. The possibility that one of the minor bands was the ALAS2 binding partner was ruled out by an analysis of the stoichiometry of binding. For example, the gel in Fig. 4*B* was digitized with an Agfa DuoScan scanner, and the bands in the 16-bit file were quantitated using ImageJ (National Institutes of Health, Bethesda, MD) and its gel analysis macros. Assuming the band staining density was proportional to protein concentration, the mol of ALAS2 bound/mol of SUCLA2 was 1.04, whereas the minor bands ranged from 0.05 to 0.4 (the band at 42 kDa was maltose-binding protein, which does not bind to ALAS2 or SUCLA2). Thus, it is highly unlikely that any of the minor bands was responsible for the observed ALAS2 binding, especially given that it has been previously shown by antibody pull-down and by yeast two-hybrid experiments that ALAS2 binds to SUCLA2 (22).

ALAS2 Affinity Chromatography of SCS—Although our studies confirm the previous association of SUCLA2 and ALAS2 (22), an alternative approach to demonstrate binding was evaluated. In a reversal of the SUCLA2 affinity chromatography experiment, wild type or M567V mutant MBP-ALAS2 fusion proteins were used as the affinity molecules instead of SUCLA2. In addition, the heterodimeric SCS holoenzyme was used as the binding partner instead of only the β subunit, SUCLA2. This experiment was performed to determine if the presence of the α subunit interfered with the binding of SUCLA2 by ALAS2 or promoted its binding to mutant ALAS2. Neither was the case because SCS bound to wild type ALAS2, as shown in Fig. 5, *lane 4*, but not to M567V (Fig. 5, *lane 5*). Quantitation of the protein bands by optical scanning of the gel showed that the SCS α and β subunit band masses were 93% of the wild type ALAS2 fusion protein band mass, indicating an ~1:1 stoichiometry between the ALAS2 homodimer and the SCS heterodimer. In contrast, the mass of the eluted SCS subunits was only 5% of the eluted M567V ALAS2 band mass, indicating very weak or nonspecific binding for the mutant enzyme. Thus, the heterodimeric SCS holoenzyme binds to wild type but not mutant ALAS2, demonstrating for the first time that the presence of the α subunit does not block this binding to the wild type enzyme; nor does it promote binding to mutant ALAS2. An unknown contaminant amounting to less than 10% of the purified SCS preparation was present in the purified SCS preparation used for the binding experiments (Fig. 5, *lane 6*). About one-third of this contaminant (relative to SCS) was recovered in the eluted material of Fig. 5, *lane 4*, indicating a loose association of this *E. coli* protein with SCS. This level of contamination was too low to be responsible for the observed 1:1 ALAS2:SCS binding stoichiometry.

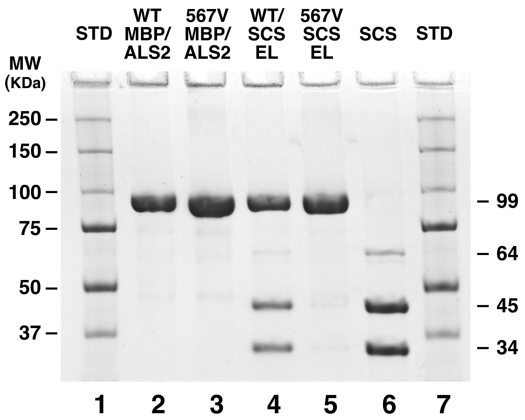

FIGURE 5. **ALAS2 affinity chromatography of SCS.** Amylose resin columns were loaded with purified recombinant human wild type or mutant MBP-ALAS2 fusion proteins and washed, and then aliquots of purified human SCS enzyme preparations were applied, washed, and then eluted with maltose as described under "Experimental Procedures." *Lanes 1* and *7*, molecular weight standards; *lane 2*, purified wild type MBP-ALAS2; *lane 3*, purified M567V mutant MBP-ALAS2; *lane 4*, material eluted by maltose from the amylose/WT MBP-ALAS2 column to which the SCS protein had been loaded and washed; *lane 5*, material eluted from an amylose/M567V MBP-ALAS2 column to which SCS had been loaded and washed; *lane 6*, purified SCS preparation that was loaded onto the columns eluted to give the material for *lanes 4* and *5*. Note that in contrast to *lane 4*, where the SCS was co-eluted with wild type ALAS2, in *lane 5*, essentially no SCS was co-eluted, and thus it failed to bind to the M567V mutant ALAS2.

In summary, rather than causing a loss of ALAS2 enzyme activity *in vitro*, these exon 11-encoded *ALAS2* mutations cause loss of binding to SUCLA2 and *in vivo* heme deficiency in XLSA patients. Furthermore, the presence of the α subunit in the heterodimeric SCS holoenzyme neither interferes with binding to wild type ALAS2 nor promotes binding to the XLSA ALAS2 mutation p.Met567Val.

Human SUCLA2 Binding to ALAS2 in XLP—An ALAS2 mutation affecting the same Met-567 residue (p.Met567GlufsX2) caused XLP instead of XLSA (17). It would be hard to reconcile overproduction of ALA and hence excess protoporphyrin IX in XLP with ALA underproduction and heme deficiency in XLSA if the p.Met567GlufsX2 ALAS2 enzyme did not bind to SUCLA2. Therefore, this mutant protein was made and tested. The homogeneous enzyme had about 2-fold greater specific activity compared with wild type ALAS2. The result in Fig. 4*D*, *lane 5*, showed that it did indeed bind to SUCLA2.

DISCUSSION

The unexpected finding that an *ALAS2* mutation in a patient with XLSA encoded a protein with completely normal enzymatic activity, kinetics, and thermostability led to the discovery

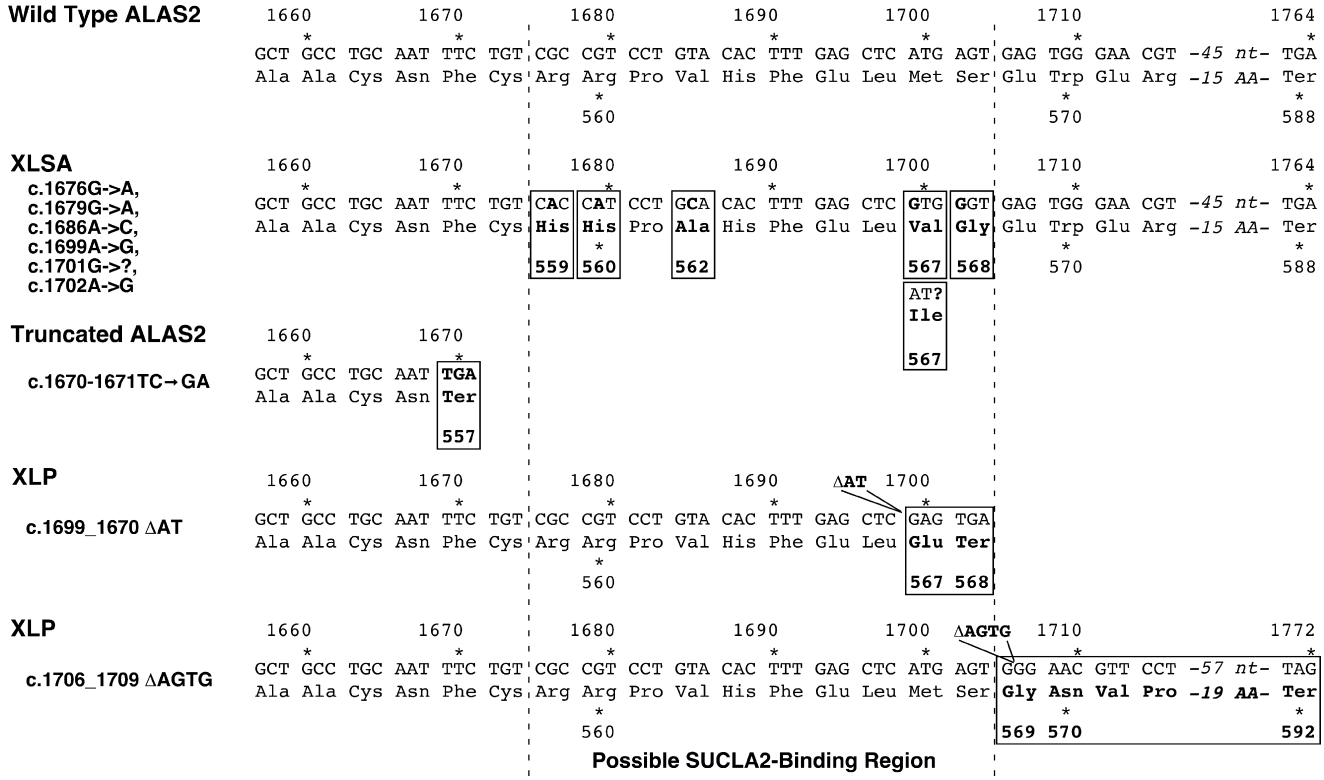

FIGURE 6. **Mutations in the ALAS2 carboxyl terminus resulting in XLSA and XLP.** Wild type and mutant ALAS2 sequences are for carboxyl-terminal amino acids beginning with ALAS2 residue Ala-553 and the corresponding cDNA nucleotides, numbering from the start codon. The 15-amino acid region at the carboxyl terminus that lacked any reported XLSA mutations is indicated in *italic type*. The mutated regions are *boxed*. The nucleotide change (c.1701G→?) was not reported for the published p.Met567Ile mutation. The *third line* shows the synthetic truncation mutation that had normal or enhanced ALAS2 activity and stability, whereas the *last two lines* show the two published ALAS2 mutations that resulted in XLP. The region where mutations may alter binding to SUCLA2 to wild type ALAS2 was confirmed by demonstration of loss of binding for XLSA mutant proteins p.Met567Val, p.Ser568Gly, and p.Phe557Ter and considered possible for the mutations at residues 559, 560, and 562 reported to result in XLSA.

that this mutation interferes with the binding of ALAS2 to the β subunit (SUCLA2) of succinyl-CoA synthetase, the enzyme that provides succinyl-CoA to ALAS2. This mechanism was confirmed by the demonstration that an adjacent XLSA mutation encoding an enzyme with normal or enhanced activity, kinetics, and stability also failed to bind to SUCLA2. Three additional XLSA-causing *ALAS2* mutations have been reported in this carboxyl-terminal region of ALAS2 (p.Arg559His (26), p.Arg560His (16, 27), p.Val562Arg (14), and p.Met567Ile (14)) as diagrammed in Fig. 6. Deletion of all of these carboxyl-terminal residues in a truncated ALAS2 protein (p.Phe557Ter, analyzed in this report) also resulted in an enzyme with normal or enhanced activity, kinetics, and stability that failed to bind to SUCLA2, consistent with mutations in this region causing XLSA by disruption of an ALAS2·succinyl-CoA synthetase complex. From the later age of onset and clinical details, where available, all of the XLSA patients with ALAS2 mutations in this region displayed a pyridoxine-responsive, mild to moderate phenotype, similar to that seen for the proband. For example, the p.Arg559His mutation was reported in an 80-year-old female, whereas the p.Arg560His mutation was found in a 36-year-old affected male and his unaffected 36-year-old brother (27). The p.Ser568Gly mutation caused anemia that did not limit physical activity, was pyridoxine-responsive *in vitro*, and resulted in 50% residual ALAS2 enzyme activity in bone marrow erythroblasts (25). The mild nature of these mutations was consistent with the fact that ALAS2 kinetics were unaffected *in vitro* and that succinyl-CoA, being an easily diffusible substrate, could still get to the enzyme, although apparently not as efficiently as when SUCLA2 was bound to ALAS2.

Importantly, the SCS holoenzyme, a heterodimer of the ALAS2-binding, ATP-utilizing β subunit, SUCLA2, and the α subunit, SULCG1, was also shown to bind to wild type ALAS2 but not to the ALAS2 mutant p.Met567Val. Thus, the presence of the alpha subunit does not prevent SCS binding to wild type ALAS2; nor does it promote binding to the mutant enzyme. Although we did not specifically test each case, we presume that SCS will behave similarly to SUCLA2 for the other mutations.

Although these results indicated that a protein-protein interaction between ALAS2 and succinyl-CoA synthetase in erythroid cell mitochondria may play a critical role in heme biosynthesis *in vivo*, the loss of SUCLA2 binding by the p.Met567Val mutant ALAS2 in the proband was perplexing because Whatley *et al.* (17) had previously shown that a two-base deletion in the *ALAS2* codon for this same residue (c.1699–1700delAT; p.Met567GlufsX2; Fig. 6) resulted in a Met to Glu change at this residue and ~40-fold greater recombinant ALAS2 activity (in crude extracts) and in XLP without anemia or iron overload. It was not obvious how the p.Met567Val mutation caused heme deficiency in XLSA due to loss of SUCLA2 binding, whereas changing this residue to glutamate and deleting the rest of the enzyme resulted in increased protoporphyrin and no anemia in XLP unless the p.Met567GlufsX2 enzyme still bound SUCLA2. Indeed, this

report demonstrated that to be true (Fig. 4*D*, *lane 5*). This may also be the case for the other known XLP mutation, c.1706–1709ΔAGTG, that caused a frameshift after Ser-568, replacing the terminal 19 amino acids with a novel 23-amino acid sequence (Fig. 6) and resulting in ~20-fold greater prokaryotically expressed mutant ALAS2 activity than wild type (17). The observation here that the homogeneous truncated mutant and the XLP mutant enzymes had at most only 2-fold elevations in ALAS2 enzymatic activity *in vitro* compared with the 20–40-fold increases previously reported for XLP deletion mutation enzymes in crude extracts suggests that *in vivo*, the relationship of these mutations to alterations in interactions with SUCLA2 or other members of a multienzyme complex may need to be considered.

Because previously reported mutations at residues 559, 560, and 562 caused XLSA although complete deletion of this region resulted in no loss of ALAS2 activity or stability, the carboxyl-terminal region from Arg-559 to Ser-568 is a possible region influencing SUCLA2 binding (Fig. 6). It should be noted, however, that although this region apparently is not required for normal ALAS2 activity and stability *in vitro*, it is still possible that the uncharacterized mutations at residues 559, 560, and 562 could negatively impact enzyme kinetics or stability *in vivo* in addition to, or instead of, loss of SUCLA2 binding. Unfortunately, predictions of ALAS2 structural interactions with SUCLA2 and of the role of this carboxyl-terminal region in XLP and XLSA are not yet possible because the only reported crystal structure (prokaryotic *Rhodobacter capsulatus* ALAS) lacks this region (31).

Of note, the first reported mutation of the *SUCLA2* gene in humans was associated with a microcytic anemia in two cousins (32). This disorder is characterized clinically primarily by encephalomyopathy, dystonia, and deafness and biochemically with succinyl-CoA overproduction, methylmalonic aciduria, and mitochondria depletion (33, 34). In contrast, microcytic anemia is absent in patients with mutations in SUCLG2, the GTP-utilizing subunit of succinyl-CoA ligase (35), previously shown not to associate with ALAS2 (22). Presumably, the genetic heterogeneity in SUCLA2 mutation patients could result from some mutations disrupting the association with ALAS2 and others not, because microcytic anemia was not a consistently reported finding. The observation that SUCLA2 did not associate with ALAS1 suggests that its unique interaction with ALAS2 is involved in an important erythroid-specific function. The presence of microcytic anemia in some SUCLA2-deficient patients, in the p.Met567Val patient reported here, in the p.Ser568Gly patient reported by Harigae *et al.* (25), and in the p.Met567Ile patient recently reported by Kadirvel *et al.* (36) all support a critical *in vivo* role for this interaction in heme biosynthesis.

Despite this evidence from multiple unrelated XLSA individuals that mutations in the carboxyl-terminal region of ALAS2 result in loss of binding to SCS, the completely normal kinetics of these mutant enzymes *in vitro* could be interpreted to indicate that some other unknown mutation(s) are actually causing XLSA in these patients. However, *in vivo* reduction in heme synthesis has now been shown to result solely from such mutations by recent experiments by Kadirvel *et al.* (36). These investigators stably overexpressed single copies of the wild type and mutant *ALAS2* genes in human HEK293 cells. They also used Western blots to show that the wild type and mutant ALAS2 enzymes were equally expressed in these cells. They found that cells expressing the wild type ALAS2 construct generated significant cellular porphyrin levels, whereas cells harboring a p.Met567Ile mutation (similar to the p.Met567Val mutation reported here, Val being of similar hydrophobicity and volume as Ile) or the same p.Ser568Gly mutation studied here, made little or no porphyrins, respectively. These results demonstrate that mutations that ablate SCS binding result in heme deficiency *in vivo*.

The involvement of ALAS2 and SCS in a multienzyme complex is possible and may be critical for additional aspects of the regulation of erythroid heme biosynthesis. Besides its interaction with ALAS2, SUCLA2 is also known to bind to nucleoside diphosphate kinase, both in prokaryotes and in eukaryotes (37, 38). Formation of an ALAS2-SUCLA complex *in vivo* is spatially reasonable because SUCLA2 is a mitochondrial matrix protein, and ALAS2 appears to be localized to the matrix side of the inner mitochondrial membrane in erythroid cells (39). Extensive additional *in vitro* and *in vivo* studies in erythroid cells may reveal further complexity once the structural and functional relationships are assessed between ALAS2, both the α and β subunits of succinyl-CoA synthetase, nucleoside diphosphate kinase, and other possible members of an apparent mitochondrial matrix/inner membrane multienzyme complex involved in erythroid heme biosynthesis. For example, the susceptibility of ALAS2 to carboxyl-terminal proteolysis (Fig. 2), coupled with the inability of the p.Phe557Ter truncated form to bind to SUCLA2 (Table 3), could provide a mechanism to regulate erythroid ALAS2 function if SUCLA2 or some other species protected ALAS2 from proteolysis *in vivo*, as suggested previously (22). Erythroid-specific proteolysis of ALAS2 has been observed using murine bone marrow cells (39). Furthermore, the precise way in which ALAS2 gain-of-function causes XLP may need to be related to ALAS2 binding to SUCLA2 in a multienzyme complex. For example, it could be that SUCLA2 binding, proteolytic sensitivity, and/or substrate supply to ALAS2 is altered in the XLP mutations, leading to a higher gain of function *in vivo* than *in vitro*.

Although the crystal structure of bacterial ALAS lacks the SUCLA2-binding carboxyl-terminal region studied here, significant insight into the reaction mechanism and structure-function relationships has been gained by alignment of mammalian ALAS2 with the bacterial sequence (used to determine the crystal structure of *R. capsulatus* ALAS), which shares 70% similarity in the catalytic core region (31, 40). In particular, a predicted loop region from approximately Ile-504 to Glu-514 containing a central Thr-508 in human ALAS2 was analogous to the loop threonine that formed a strong hydrogen bond to the carboxyl group of succinyl-CoA in the bacterial crystal structure. This loop has been shown to play a key role in regulating the catalytic rate of the murine enzyme (40, 41). Hunter and Ferreira (40) have proposed that this loop's conformation could be modulated by binding of small molecules or succinyl-CoA synthetase in this region, thus controlling enzyme activity. Similarly, it can be speculated that the ALAS2 carboxyl-termi-

nal mutations seen in XLP that result in increased protoporphyrin production function to alter the structure and/or position of the carboxyl-terminal region of ALAS2 such that it permits substrates easier access to the active site, thus increasing enzymatic activity.

The present report demonstrates that in two XLSA patients, the causative p.Met567Val and p.Ser568Gly mutations in this more distal carboxyl-terminal region eliminate the binding of succinyl-CoA synthetase to ALAS2. Additional *in vivo* studies are needed to determine if the reduction of heme synthesis in these patients is only due to loss of contact between ALAS2 and SUCLA2 or is mediated through alterations in the Thr-508 active site loop, increased susceptibility of ALAS2 to protease, altered compartmentalization of ALAS2, or other processes.

The carboxyl-terminal domain of human ALAS2 following Cys-555 is probably a eukaryotic invention because it is notably missing in prokaryotes. The region where mutations alter the binding of ALAS2 to SUCLA2 (Fig. 6) and the remaining carboxyl-terminal residues are quite conserved in eukaryotes and thus may be important for an erythroid-specific function unneeded in prokaryotes. Further *in vivo* studies of a multienzyme complex involving ALAS2 will probably be important for a full understanding of the pathogenesis of certain types of XLSA and of XLP.

Acknowledgments—We acknowledge the Mount Sinai Mass Spectrometry Proteomic Laboratory (Dr. Ron Wang, director) for ALAS2 peptide analyses. We thank I. Nazarenko for constructing the ALAS2 ΔAT clone and thank Drs. James Wetmur and Robert J. Desnick for comments on drafts of the manuscript.

REFERENCES

1. Bishop, D. F., Henderson, A. S., and Astrin, K. H. (1990) Human δ-aminolevulinate synthase. Assignment of the housekeeping gene to 3p21 and the erythroid-specific gene to the X chromosome. *Genomics* **7,** 207–214
2. Anderson, K. E., Sassa, S., Bishop, D. F., and Desnick, R. J. (2001) Disorders of heme biosynthesis. X-linked sideroblastic anemia and the porphyrias. in *The Metabolic and Molecular Bases of Inherited Disease*, 8th Ed. (Scriver, C. R., Beaudet, A. L., Sly, W. S., Valle, D., Childs, B., Kinzler, K. W., and Vogelstein, B., eds) pp. 2991–3062, McGraw-Hill, New York
3. Ferreira, G. C., Neame, P. J., and Dailey, H. A. (1993) *Prot. Sci.* **2,** 1959–1965
4. Ferreira, G. C., Vajapey, U., Hafez, O., Hunter, G. A., and Barber, M. J. (1995) Aminolevulinate synthase. Lysine 313 is not essential for binding the pyridoxal phosphate cofactor but is essential for catalysis. *Protein Sci.* **4,** 1001–1006
5. Cotter, P. D., Baumann, M., and Bishop, D. F. (1992) Enzymatic defect in "X-linked" sideroblastic anemia. Molecular evidence for erythroid δ-aminolevulinate synthase deficiency. *Proc. Natl. Acad. Sci. U.S.A.* **89,** 4028–4032
6. Cox, T. C., Bottomley, S. S., Wiley, J. S., Bawden, M. J., Matthews, C. S., and May, B. K. (1994) X-linked pyridoxine-responsive sideroblastic anemia due to a Thr-388 to Ser substitution in erythroid 5-aminolevulinate synthase. *New Engl. J. Med.* **330,** 675–679
7. Camaschella, C. (2008) Recent advances in the understanding of inherited sideroblastic anaemia. *Br. J. Haematol.* **143,** 27–38
8. Cotter, P. D., Rucknagel, D. L., and Bishop, D. F. (1994) X-linked sideroblastic anemia. Identification of the mutation in the erythroid-specific δ-aminolevulinate synthase gene (*ALAS2*) in the original family described by Cooley. *Blood* **84,** 3915–3924
9. Cotter, P. D., May, A., Fitzsimons, E. J., Houston, T., Woodcock, B. E., al-Sabah, A. I., Wong, L., and Bishop, D. F. (1995) Late onset X-linked sideroblastic anemia. Missense mutations in the erythroid δ-aminolevulinate synthase (*ALAS2*) gene in two pyridoxine-responsive patients initially diagnosed with acquired refractory anemia and ringed sideroblasts. *J. Clin. Invest.* **96,** 2090–2096
10. Furuyama, K., Harigae, H., Heller, T., Hamel, B. C., Minder, E. I., Shimizu, T., Kuribara, T., Blijlevens, N., Shibahara, S., and Sassa, S. (2006) Arg-452 substitution of the erythroid-specific 5-aminolevulinate synthase, a hot spot mutation in X-linked sideroblastic anemia, does not itself affect enzyme activity. *Eur. J. Haematol.* **76,** 33–41
11. Cotter, P. D., May, A., Li, L., Al-Sabah, A. I., Fitzsimons, E. J., Cazzola, M., and Bishop, D. F. (1999) Four new mutations in the erythroid-specific 5-aminolevulinate synthase (*ALAS2*) gene causing X-linked sideroblastic anemia. Increased pyridoxine responsiveness after removal of iron overload by phlebotomy and coinheritance of hereditary hemochromatosis. *Blood* **93,** 1757–1769
12. May, A., and Bishop, D. (1998) The molecular biology and pyridoxine responsiveness of X-linked sideroblastic anemia. *Haematologica* **83,** 56–70
13. Bottomley, S. S. (2009) Sideroblastic anemias. in *Wintrobe's Clinical Hematology* (Greer, J. P., Foerster, J., Rodgers, G. M., Paraskevas, F., Blader, B., Arber, D. A., and Means, R. T., Jr., eds) pp. 835–856, Wolters Kluwer/Lippincott Williams & Wilkins, Philadelphia
14. Harigae, H., and Furuyama, K. (2010) Hereditary sideroblastic anemia. Pathophysiology and gene mutations. *Int. J. Hematol.* **92,** 425–431
15. Collins, T. S., and Arcasoy, M. O. (2004) Iron overload due to X-linked sideroblastic anemia in an African American man. *Am. J. Med.* **116,** 501–502
16. Lee, P. L., Barton, J. C., Rao, S. V., Acton, R. T., Adler, B. K., and Beutler, E. (2006) Three kinships with ALAS2 P520L (c.1559C→T) mutation, two in association with severe iron overload and one with sideroblastic anemia and severe iron overload. *Blood Cells Mol. Dis.* **36,** 292–297
17. Whatley, S. D., Ducamp, S., Gouya, L., Grandchamp, B., Beaumont, C., Badminton, M. N., Elder, G. H., Holme, S. A., Anstey, A. V., Parker, M., Corrigall, A. V., Meissner, P. N., Hift, R. J., Marsden, J. T., Ma, Y., Mieli-Vergani, G., Deybach, J. C., and Puy, H. (2008) C-terminal deletions in the *ALAS2* gene lead to gain of function and cause X-linked dominant protoporphyria without anemia or iron overload. *Am. J. Hum. Genet.* **83,** 408–414
18. Urata, G., and Granick, S. (1963) Biosynthesis of α-aminoketones and the metabolism of aminoacetone. *J. Biol. Chem.* **238,** 811–820
19. Mauzerall, D., and Granick, S. (1956) The occurrence and determination of δ-aminolevulinic acid and porphobilinogen in urine. *J. Biol. Chem.* **219,** 435–446
20. Bishop, D. F., Wampler, D. E., Sgouris, J. T., Bonefeld, R. J., Anderson, D. K., Hawley, M. C., and Sweeley, C. C. (1978) Pilot scale purification of α-galactosidase A from Cohn fraction IV-1 of human plasma. *Biochim. Biophys. Acta* **524,** 109–120
21. Bertoldi, M., Cellini, B., Laurents, D. V., and Borri Voltattorni, C. (2005) Folding pathway of the pyridoxal 5′-phosphate C-S lyase MalY from *Escherichia coli*. *Biochem. J.* **389,** 885–898
22. Furuyama, K., and Sassa, S. (2000) Interaction between succinyl-CoA synthetase and the heme-biosynthetic enzyme ALAS-E is disrupted in sideroblastic anemia. *J. Clin. Invest.* **105,** 757–764
23. Cox, T. C., Sadlon, T. J., Schwarz, Q. P., Matthews, C. S., Wise, P. D., Cox, L. L., Bottomley, S. S., and May, B. K. (2004) The major splice variant of human 5-aminolevulinate synthase-2 contributes significantly to erythroid heme biosynthesis. *Int. J. Biochem. Cell Biol.* **36,** 281–295
24. Segel, I. H. (1975) *Enzyme Kinetics*, pp. 360–368, John Wiley & Sons, Inc., New York
25. Harigae, H., Furuyama, K., Kimura, A., Neriishi, K., Tahara, N., Kondo, M., Hayashi, N., Yamamoto, M., Sassa, S., and Sasaki, T. (1999) A novel mutation of the erythroid-specific δ-aminolevulinate synthase gene in a patient with X-linked sideroblastic anemia. *Br. J. Haematol.* **106,** 175–177
26. Pereira, J. C., Goncalves, P., Cuhna, E., and Ribeiro, M. L. (2004) Gene symbol, *ALAS2*. Disease, sideroblastic anemia. *Hum. Genet.* **115,** 533
27. Cazzola, M., May, A., Bergamaschi, G., Cerani, P., Ferrillo, S., and Bishop, D. F. (2002) Absent phenotypic expression of X-linked sideroblastic anemia in one of two brothers with a novel ALAS2 mutation. *Blood* **100,**

4236–4238
28. Bottomley, S. S., May, B. K., Cox, T. C., Cotter, P. D., and Bishop, D. F. (1995) Molecular defects of erythroid 5-aminolevulinate synthase in X-linked sideroblastic anemia. *J. Bioenerg. Biomembr.* **27,** 161–168
29. Koc, S., Bishop, D. F., Li, L., Danish, E. H., Brittenham, G. M., and Harris, J. W. (1997) Iron overload in pyridoxine-responsive X-linked sideroblastic anemia: Greater severity in a heterozygote than in her hemizygous brother. *Blood* **90,** Suppl 1, 2756A
30. Hunter, G. A., and Ferreira, G. C. (1999) Pre-steady-state reaction of 5-aminolevulinate synthase. Evidence for a rate-determining product release. *J. Biol. Chem.* **274,** 12222–12228
31. Astner, I., Schulze, J. O., van den Heuvel, J., Jahn, D., Schubert, W. D., and Heinz, D. W. (2005) Crystal structure of 5-aminolevulinate synthase, the first enzyme of heme biosynthesis, and its link to XLSA in humans. *EMBO J.* **24,** 3166–3177
32. Elpeleg, O., Miller, C., Hershkovitz, E., Bitner-Glindzicz, M., Bondi-Rubinstein, G., Rahman, S., Pagnamenta, A., Eshhar, S., and Saada, A. (2005) Deficiency of the ADP-forming succinyl-CoA synthase activity is associated with encephalomyopathy and mitochondrial DNA depletion. *Am. J. Hum. Genet.* **76,** 1081–1086
33. Ostergaard, E., Hansen, F. J., Sorensen, N., Duno, M., Vissing, J., Larsen, P. L., Faeroe, O., Thorgrimsson, S., Wibrand, F., Christensen, E., and Schwartz, M. (2007) Mitochondrial encephalomyopathy with elevated methylmalonic acid is caused by SUCLA2 mutations. *Brain* **130,** 853–861
34. Carrozzo, R., Dionisi-Vici, C., Steuerwald, U., Lucioli, S., Deodato, F., Di Giandomenico, S., Bertini, E., Franke, B., Kluijtmans, L. A., Meschini, M. C., Rizzo, C., Piemonte, F., Rodenburg, R., Santer, R., Santorelli, F. M., van Rooij, A., Vermunt-de Koning, D., Morava, E., and Wevers, R. A. (2007) *Brain* **130,** 862–874
35. Valayannopoulos, V., Haudry, C., Serre, V., Barth, M., Boddaert, N., Arnoux, J. B., Cormier-Daire, V., Rio, M., Rabier, D., Vassault, A., Munnich, A., Bonnefont, J. P., de Lonlay, P., Rötig, A., and Lebre, A. S. (2010) New SUCLG1 patients expanding the phenotypic spectrum of this rare cause of mild methylmalonic aciduria. *Mitochondrion* **10,** 335–341
36. Kadirvel, S., Furuyama, K., Harigae, H., Kaneko, K., Tamai, Y., Ishida, Y., and Shibahara, S. (2012) The carboxyl-terminal region of erythroid-specific 5-aminolevulinate synthase acts as an intrinsic modifier for its catalytic activity and protein stability. *Exp. Hematol.* **40,** 477–486.e1
37. Kadrmas, E. F., Ray, P. D., and Lambeth, D. O. (1991) Apparent ATP-linked succinate thiokinase activity and its relation to nucleoside diphosphate kinase in mitochondrial matrix preparations from rabbit. *Biochim. Biophys. Acta* **1074,** 339–346
38. Kavanaugh-Black, A., Connolly, D. M., Chugani, S. A., and Chakrabarty, A. M. (1994) Characterization of nucleoside-diphosphate kinase from *Pseudomonas aeruginosa*. Complex formation with succinyl-CoA synthetase. *Proc. Natl. Acad. Sci. U.S.A.* **91,** 5883–5887
39. Dzikaite, V., Kanopka, A., Brock, J. H., Kazlauskas, A., and Melefors, O. (2000) A novel endoproteolytic processing activity in mitochondria of erythroid cells and the role in heme synthesis. *Blood* **96,** 740–746
40. Hunter, G. A., and Ferreira, G. C. (2011) Molecular enzymology of 5-aminolevulinate synthase, the gatekeeper of heme biosynthesis. *Biochim. Biophys. Acta* **1814,** 1467–1473
41. Lendrihas, T., Hunter, G. A., and Ferreira, G. C. (2010) Targeting the active site gate to yield hyperactive variants of 5-aminolevulinate synthase. *J. Biol. Chem.* **285,** 13704–13711